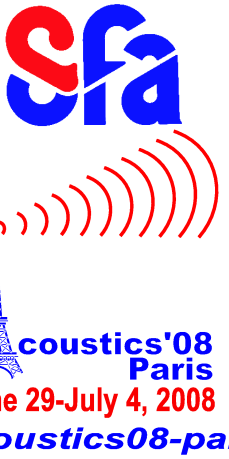

euronoise

Active noise control in light jet aircraft

Oliver Pabst, Thomas Kletschkowski and Delf Sachau

Helmut-Schmidt-Universität - Universität der Bundeswehr Hamburg, Holstenhofweg 85, 22043 Hamburg, Germany
opabst@hsu-hh.de

Active systems for noise reduction are especially of interest when considering applications in which low-frequency noise is a main source of disturbance and only limited amounts of installation space and payload are available. This makes the adaptation and implementation of such systems plausible in vehicles such as automobiles and aircraft where passive reduction methods are restricted. In order to achieve effective active control in these environments, aspects such as the control method and actuator- and sensor type as well as positioning must be considered. The noise characteristics are often known beforehand or are accessible by measurement. Using this data, an upper bound for possible noise reduction may be determined, e.g. by means of linear prediction methods. A current research project is aimed at developing an audio-system for the cabin area of a light jet aircraft which, at the same time, should also function as an effective noise reduction system in order to enhance the cabin comfort as well as the audio quality. Using data from a measurement flight in a typical light jet aircraft, limitations of active control are determined. Furthermore, the test bed, an acoustic mock-up, is presented, currently beholding a multi-channel ANC-Audio system for tonal and broadband noise.

1 Introduction

Reducing interior noise levels in passenger aircraft has been a focus of research in active control for many years [1, 2, 3]. This is due to the fact that propeller-driven aircraft are prone to high noise levels which are related to the blade passage frequency (BPF). Since a highly correlated reference signal is accessible by monitoring the engine(s), active noise reduction in propeller aircraft has been a typical subject of feedforward control. For jet aircraft suitable algorithms and control strategies are yet to be found since many complex sources such as boundary layer noise and turbine-induced jet noise are involved in creating the disturbance in the cabin [4].

Considering the current growth of the light jet market, the reduction of broadband noise in small jet aircraft has become of interest, giving rise to new fields of research. Due to small cabin sizes in the range of larger automobiles (typical van), active noise control (ANC) systems for small jet aircraft may retain a feasible effort in terms of algorithm complexity and system topology. However, an active system, especially in such small aircraft, should not create excessive payload nor should it take up much space. Consequently, the combination of noise control with an integrated audio system may be deemed a reasonable combination.

A current research project at the Mechatronics Department of the Helmut-Schmidt-University (HSU) is aimed at developing such an audio-system for the cabin area of a small jet aircraft which, at the same time, should also function as an effective noise reduction system in order to enhance the cabin comfort as well as the audio quality [5]. The system is to be integrated and tested in the interior of an acoustic mock-up, which is fabricated by the industrial project partner “Innovint, Aircraft Interior GmbH”.

Measurements taken during a flight in a typical light jet aircraft are briefly introduced in the following section with regard to ANC profit limits. Section 3 focuses on developing an ANC system using the modified filtered-X least mean square algorithm (mFx-LMS) for tonal and broadband noise. Here, a closer look will be taken into controlling a realistic primary disturbing sound field as well as into integrated audio in the controller.

2 Cabin Noise Characteristics

In order to determine typical cabin noise in light jets, numerous measurements were done in a Cessna Citation Bravo (6 seats, lounge configuration) [5]. Five fixed microphone positions (at the approx. head position of a passenger) to record during the entire flight and five microphones in an array to map the sound field of the cabin area during the cruise condition were used (s. Fig. 1). The mapping was done at 24000ft with 268KIAS (indicated air speed in knots). White spaces were left in areas, where no measurements were possible.

The general spectral shape of the recorded data during cruise (s. Fig. 1 b), Mic. 3) is broadband colored noise with a rise at frequencies between 50Hz - 200Hz as well as frequencies around 400Hz. The former decreases with distance from the rear cabin area. The main contribution of the cabin noise is below 1kHz which, in general, implies that this is a feasible application for active noise control. Total sound pressure levels (SPL) of 85dB – 95dB were measured. The lowest SPLs were at the center of the front cabin and the highest at rear positions close to the fuselage as shown in Fig. 1 a).

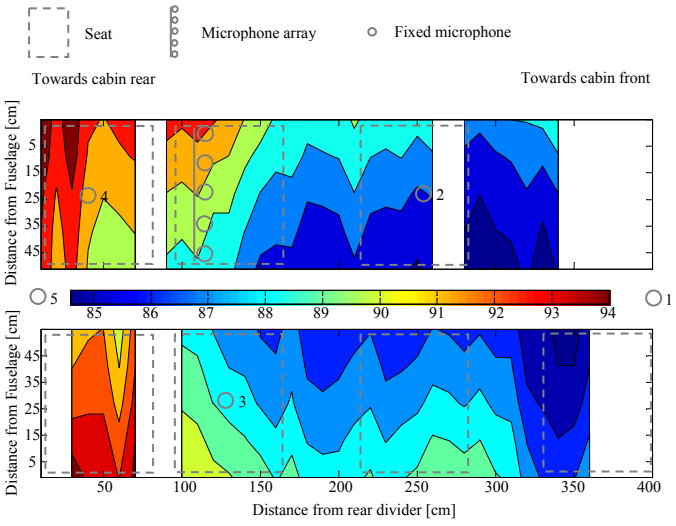

a) Mapping of the total cabin SPL in dB during cruise for the left (top) and right (bottom) cabin halves. Mics. 1 and 5 were placed in the gangway.

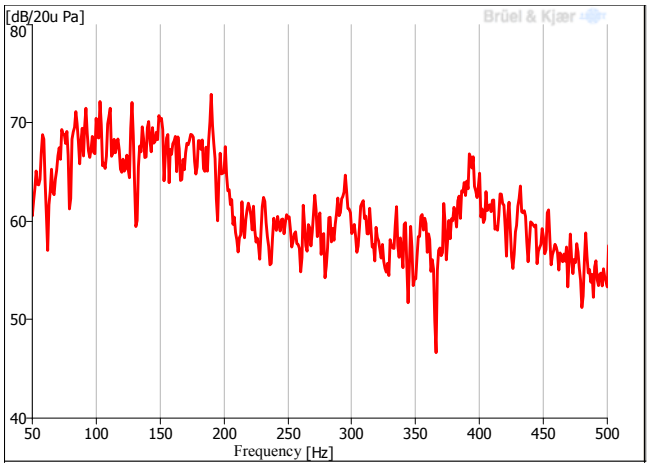

b) Typical spectral shape during cruise (SPL at Mic. 3 of Fig. 1a)).

Fig. 1 Result of measurements in a typical light jet.

2.1 Prediction of ANC Bounds

In the case of feedforward control concepts, a well known measure for an upper bound of possible control profit with stationary noise signals is the coherence between the reference signal and the error signal [6]. The coherence between different fixed microphone locations during the cruise flight state was measured in order to see if these could serve as possible reference positions. Analysis results show that these signals would not suffice as a reference for a feedforward controller as the coherence value at most considered frequencies (f < 500Hz) is far below 0.7 resulting in an upper bound of 4-5dB of possible reduction per frequency [6].

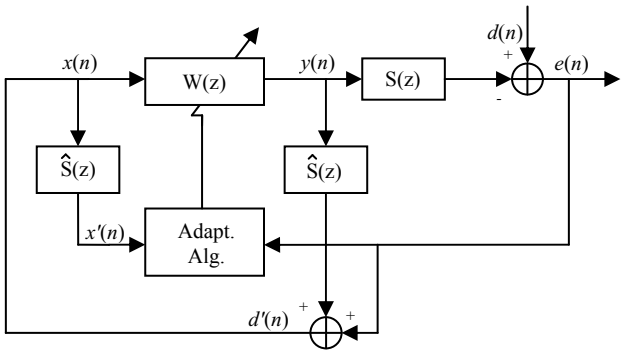

Fig. 2 Feedback controller with reference signal synthesis and Fx-structure.

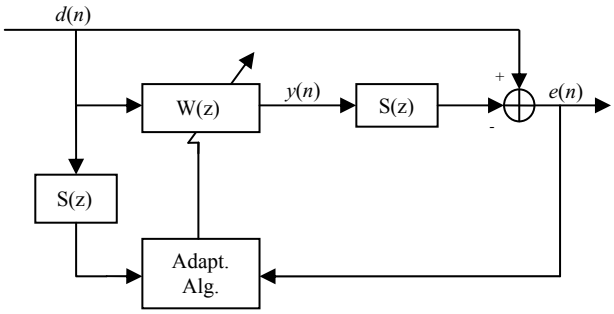

Fig. 3 The feedback controller of Fig. 2 takes on a feedforward form for $S = \hat{S}$.

A different approach to the prediction of an upper bound for ANC profit is given by means of linear prediction. Fig. 2 shows a broadband feedback controller for active noise control with reference signal synthesis and a filtered-x algorithm for adaptation. Here, $S(z)$ denotes the secondary path transfer function representing the physical path from the D/A (digital to analog) conversion at the controller output to the A/D (analog to digital) conversion of the error microphone signal at the controller input. If the secondary path model $\hat{S}(z)$ is assumed to be equal to the secondary path, $\hat{S}(z) = S(z)$, the estimate $d'(n) = d(n)$ and therefore, $x(n) \equiv d(n)$. Under these conditions, the controller in Fig. 2 may be modified as displayed in Fig. 3. Now, assuming that the coefficients of the adaptive filter vary slowly, $W(z)$ and $S(z)$ may be switched, leaving only one $S(z)$ in front of the branch to the adaptive filter and adaptation algorithm. In a final generalization, $S(z)$ is assumed to be a pure delay $S = z^{-\Delta}$ resulting in a prediction error filter [7] as in Fig. 4 with

$$\begin{aligned} E(z) &= D(z) - Y(z) \\ &= D(z) - z^{-\Delta}D(z)W(z) \\ &= [1 - z^{-\Delta}W(z)]\, D(z) \\ E(z)/D(z) &= [1 - z^{-\Delta}W(z)]. \end{aligned} \quad (1)$$

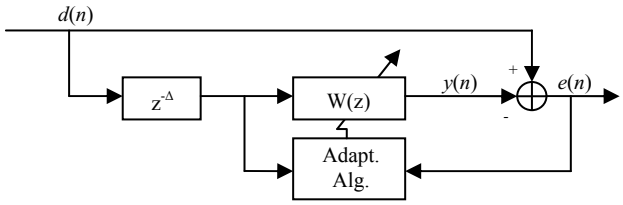

Fig. 4 Prediction error filter.

For the given assumptions, the adaptive feedback controller turns into a prediction error filter whose control profit is governed by the predictability of $d(n)$.

Now, considering a feedforward ANC controller as in Fig. 5, the error signal $e(n)$ is also dependent on the transfer function between the noise source an the error microphone, known as the primary path $P(z)$:

$$\begin{aligned} E(z) &= D(z) - Y(z)S(z) \\ &= P(z)X(z) - W(z)\, X(z)S(z) \\ &= [P(z) - W(z)S(z)]\, X(z) \\ E(z)/D(z) &= [1 - W(z)S(z)/P(z)]. \end{aligned} \quad (2)$$

The relation $E(z)/D(z)$ for feedforward ANC and the predictor is equal if

$$\begin{aligned} [1 - z^{-\Delta}W_{LP}(z)] &= [1 - W_{FF}(z)S(z)/P(z)] \\ z^{-\Delta}W_{LP}(z) &= W_{FF}(z)S(z)/P(z) \\ W_{FF}(z) &= z^{-\Delta}W_{LP}(z)P(z)/S(z), \end{aligned} \quad (3)$$

where *FF* denotes the feedforward filter and *LP* denotes the prediction filter. It may be seen that a statement towards noise reduction capabilities with a feedforward structure can be made via simulation with a prediction error filter if further information on the primary path (i.e. an estimate) is accessible. Assuming that the primary path is a pure delay and that the secondary path is negligible Eq. (3) can be written as

$$W_{FF}(z) = z^{-(\Delta+\Delta p)} W_{LP}(z) \tag{4}$$

with Δ_p as the delay due to the primary path.

Results of this analysis for a signal recorded at a fixed microphone position (s. Fig. 1, Mic. 3) during flight (cruise) for $\Delta = 1$ with a prediction error filter length of 50 and a sampling frequency of 16kHz show that 22dB or 30dBA are possible for $50\text{Hz} < f < 500\text{Hz}$. As this assumes greatest simplification, it represents the expected upper bound for real noise reduction capabilities.

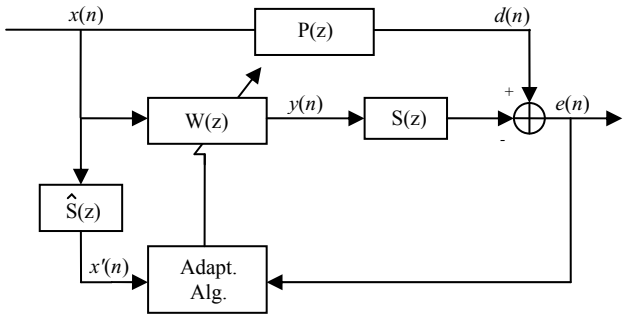

Fig. 5 Feedforward controller for ANC with Fx-structure.

3 Active Noise Control

In order to test the feasibility of ANC in a small jet aircraft, an experimental ANC system with variable actuator- and microphone positions as well as quantities was installed in an acoustic mock-up. The wooden mock-up currently beholds a simplified cabin interior made of foam and wood. Original cabin materials were used for the lining, carpets and seats. Simplifications were made for the avionics in the cockpit as well as in the seats [5]. This first stage of the mock-up also does not yet have windows (s. Fig. 9). However, these will be added in future.

Different control algorithms have been tested in the mock-up including the filtered-x least mean square algorithm (Fx-LMS) and the modified Fx-LMS [8]. In the following sections, a closer look shall be taken at the modified structure as well as considerations towards an audio integrated ANC system.

3.1 The modified Fx-LMS Algorithm

In feedforward noise control systems, the Fx-LMS algorithm is widely used due to its stability and is well understood. However slow convergence is possible considering that the delay of the secondary path Δ limits the step size to $\mu = 2/(L \cdot \Delta \cdot P_x)$, where L is the controller filter-length and P_x is the power of the reference signal [9]. Furthermore, an adaptation of the filtered-x structure to accommodate more sophisticated algorithms than the LMS, such as the recursive least square (RLS) or Kalman filter based algorithms proves complex.

These effects may be avoided by using an alternative feedforward structure as shown in Fig. 6. This modified structure uses a model of the secondary path to derive an estimate of the primary disturbance $d'(n)$. This estimate is then used to generate a new error signal $e_m(n)$ for the adaptation process. $e_m(n)$ is directly dependent on changes in the adaptive Filter $W(z)$ [9]. Filter coefficients are copied to the controller. The step-size and therefore the convergence speed are no longer dependent on the secondary path delay for well modeled path estimates.

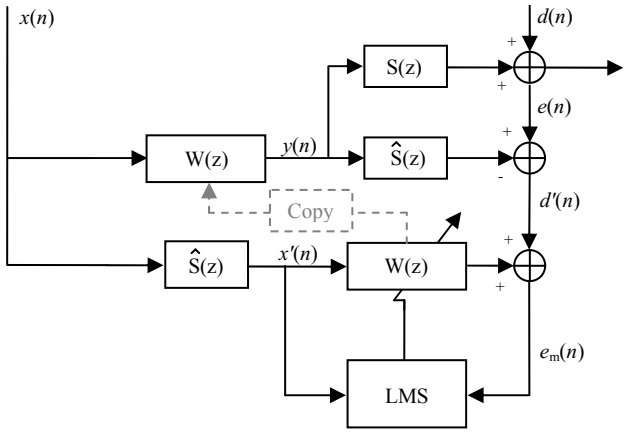

Fig. 6 Block-diagram of the modified Fx-LMS algorithm for ANC.

Following the description in Fig. 6, the modified filtered-x LMS algorithm for ANC can be described by:

$$d'(n) = e(n) - \sum_{j=1}^{J} \hat{s}_j \cdot y(n-j)\,, \tag{5}$$

$$e_m(n) = d'(n) + \sum_{l=0}^{L-1} \sum_{j=0}^{J-1} w_l(n) \cdot \hat{s}_j \cdot x(n-l-j)\,, \tag{6}$$

$$\mathbf{w}(n+1) = \mathbf{w}(n) - \mu \cdot \mathbf{x}'(n) \cdot e_m(n) \tag{7}$$

with J as the number of secondary path model coefficients and $\mathbf{w}(n)$ being the column-matrix of adaptive filter coefficients. $\mathbf{x}'(n)$ is the column-matrix of filtered reference signals.

The adaptation of these equations to a multichannel algorithm as used in the following experiments is equivalent to that of the Fx-LMS and has previously been presented in [8].

3.2 ANC + Audio

As previously mentioned, the in-flight audio system and the active noise control system are to be merged. This is done for the low-frequency components of the audio signal which could simply be added to the controller output.

However, two main issues arise in this case. The reproduced audio may interfere with the ANC system and hinder a correct adaptation of the filter and furthermore, the ANC system may also cancel the audio signal as well as the disturbing noise. In order to guarantee a high quality audio experience in the passenger area, the error signal must be freed of audio signal components before being used in the filter adaptation process. This can be done in a straightforward manner as shown in the block diagram of the modified Fx-LMS with audio in Fig. 7. The preamplified audio signal is added to the cancellation signal resulting in $y_a(n)$ and, due to the modified structure, is subtracted from the error signal along with the cancellation signal. The extra secondary path model which is required for the audio compensating Fx-LMS algorithm [6] is already contained in the modified structure as described in the preceding section.

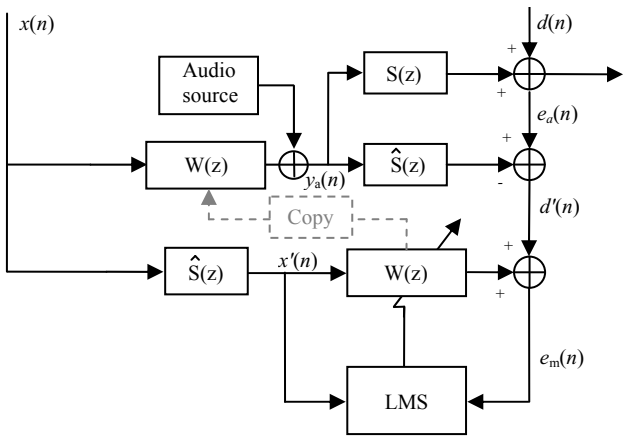

Fig. 7 Block-diagram of the modified Fx-LMS algorithm for ANC with audio.

Considering that $y_a(n)$ is the sum of audio and controller output, then the z transform of the error signal $e_a(n)$ is given by

$$E_a(z) = D(z) + Y_a(z)S(z) \tag{8}$$

and

$$\begin{aligned} D'(z) &= E_a(z) - Y_a(z)\hat{S}(z) \\ &= D(z) + Y_a(z)S(z) - Y_a(z)\hat{S}(z). \end{aligned} \tag{9}$$

For negligible errors in the secondary path and under the assumption that the audio signal is not correlated with reference signal, $d'(n) = d(n)$, as without audio.
An interesting aspect of a controller integrated audio reproduction system is the possibility of using this feature for online secondary path modeling. Such a system would regularly adapt the secondary path model e.g. compensating for changes in the cabin area, such as more passengers or luggage. The online method will be a part of future work.

3.3 Experimental Results

Using a dSPACE hardware platform (type 1006, 2.6Ghz, I/O 16 bit), the mFx-LMS was implemented in power-normalized and leaky forms [6] with offline plant modelling of the secondary paths. A primary noise field was generated by a loudspeaker which was also placed inside of the cabin. For these experiments the noise generator signal was directly passed through to the controller (internal reference). The multichannel system was tested in 1x6x8 setup (reference x loudspeakers x microphones) with positions as shown in Fig. 8 and Fig. 9. The microphones are positioned in the headrests of the seats at approx. expected passenger ear positions and are numbered 1-8. Rear speakers are above the passenger head in the rear divider. The other four positions are on the floor between the seats and underneath the first two seats.

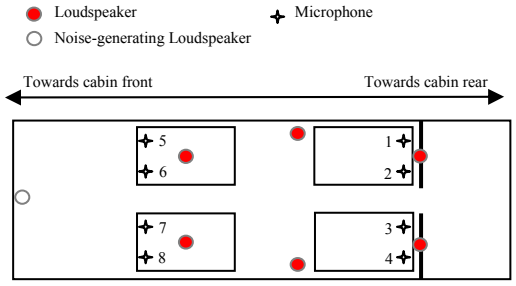

Fig. 8 Microphone-/ speaker positions in the mock-up.

Fig. 9 Acoustic mock-up interior with the experimental ANC system (view towards cabin rear from 1. seat row).

Experimental results of the Fx-LMS are not further discussed as upcoming work is focussed on the mFx-LMS algorithm for reasons described in the previous section.

Experiments with the mFx-LMS were done with band limited white noise (20Hz < f < 500Hz) at 35dB total SPL above ambient SPL as a primary disturbance. Fig. 10 shows the effect of active control in the considered frequency band for microphone position 1 (410 filtertaps for all filters). Control results at the other positions may be taken from Table 2. As a first step towards controlling a more realistic disturbance in terms of its characteristics, another broadband ANC experiment was performed using a recorded signal from the previously described flight in a Cessna Citation Bravo. The results are shown in Table 3.

Low-frequency audio reproduction was integrated into the ANC system. The low pass filtered audio signal was fed into the controller as described in section 3.2 without noticeable loss of noise reduction capabilities.

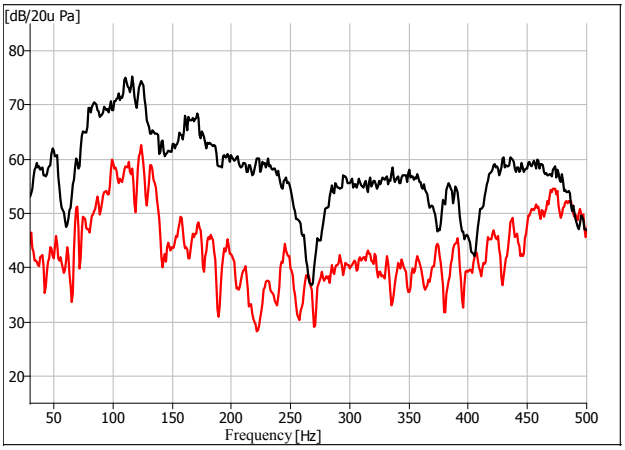

Fig.10 Broadband ANC with the multichannel mFx-LMS at one microphone position. SPL with ANC off (black), SPL with ANC on (red).

Microphone Nr.	Total Pressure (ANC off) [dB]	Total Pressure (ANC on) [dB]	Delta [dB]
1	88.49	74.32	14.17
2	87.09	76.65	10.44
3	86.70	74.32	12.38
4	88.02	73.60	14.42
5	88.19	78.19	10.00
6	87.87	75.49	12.38
7	87.85	75.85	12.00
8	88.13	77.49	10.64

Table 2 Real-time noise cancellation at the error microphones for broadband noise (20Hz < f < 500Hz).

Microphone Nr.	Total Pressure (ANC off) [dB]	Total Pressure (ANC on) [dB]	Delta [dB]
1	89.68	77.38	12.3
2	88.23	80.01	8.22
3	87.73	75.97	11.76
4	89.16	75.28	13.88
5	89.46	78.99	10.47
6	89.23	75.96	13.27
7	89.11	77.04	12.07
8	89.23	77.41	11.82

Table 3 Real-time noise cancellation at the error microphones for broadband noise recorded in a light jet.

4 Conclusion

In summary, for the given generalizations, a first impression of ANC capabilities in terms of an upper bound may be acquired by means of a prediction error filter also for feedforward algorithms. The convenience of this is that a recorded sample of the disturbance may be analyzed without further information on primary- or secondary paths. Using data from measurements performed during flight in a typical light jet, these upper bounds were determined. Initial steps in developing a combined active noise- and audio system for a (very) light jet aircraft with the multichannel modified Fx-LMS were introduced. Using the modified Fx-LMS variant simplifies the audio integration step without further workload for the controller. First results of multichannel active noise control with the mFx-LMS for broadband disturbances were presented. Broadband disturbances taken from a real measurement flight were also subjected to ANC testing. A combined low-frequency audio reproduction and ANC system was implemented and shown to be functional.

Acknowledgments

Funding by the City of Hamburg in the framework of LuFoHH to enable this project is gratefully acknowledged.

References

[1] Elliott, S. J.; Nelson, P. A.; Stothus, L. M.; Boucher, C. C.: “In-flight Experiments on the Active Control of Preopeller-induced Cabin Noise”, *J. Sound and Vibration.* 140(2), 219-238 (1990)

[2] Johansson, S.; Lago, T.; Nordebo, S.; Claesson, I.: “Control Approaches for Active Noise Control of Propeller-induced Cabin Noise evaluated from Data from a Dornier 328 Aircraft”, *In Proc. 6th int. Congress on Sound and Vibration, Copenhagen,* p. 1611-1618 (1999)

[3] Borchers, I. U.; Emborg, U.; Sollo, A.; Waterman, E. H.; Paillard, J.; Larsen, P. N. Venet, G.; Goeransson, P.; Martin, V.: “Advanced Study for Active Noise Control in Aircraft (ASANCA)”, *Fourth Aircraft Interior Noise Workshop, NASA Langley Research Center, USA,* p. 129-141, July (1997)

[4] Wilby, J. F.: “Aircraft Interior Noise”, *J. Sound and Vibration.* 190(3), 545-564 (1996)

[5] Pabst, O.; Kletschkowski, T.; Sachau, D.: “Audio Interior for Light Aircraft“, *In Proc. Deutscher Luft- und Raumfahrt Kongress (CEAS), Berlin,* Sept. (2007)

[6] Kuo, S. M., Morgan, D. R.: “Active Noise Control Systems, Algorithms and DSP Implementations”, *New York, NY.: Wiley,* ISBN 0471134244 (1996)

[7] Haykin, S.: “Adaptive Filter Theory”, *Upper Saddle River, N.J.: Prentice Hall, Inc.,* ISBN 0130484342 (2002)

[8] Bouchard, M., Quednau, S.: “Multichannel Recursive-Least-Squares Algorithms and Fast-Transversal-Filter Algorithms for Active Noise Control and Sound Reproduction Systems”, *IEEE Trans. Speech and Audio Processing,* Vol. 8, No. 5, 606-618, Sept. (2000)

[9] Elliot, S. J.: “Signal Processing for Active Control”, *San Diego, CA.: Academic Press,* ISBN 0122370856 (2001)